Materials and Methods

Reagents and Antibodies

Matrigel™ Basement Membrane Matrix was from BD Biosciences Discovery Labware, EGF from Upstate/Millipore, Cariporide was kindly gifted from Aventis Pharma and Erlotinib from Genentech, Inc. Rabbit policlonal antibody against EGFR (D38B1) was from Cell Signaling Technology, rabbit EGFR (phospho-Tyr1173) antibody from GeneTex, mouse monoclonal against NHERF1 was from BD Transduction Laboratories, rabbit policlonal antibody against NHERF1 was from Affinity Bio Reagents, rabbit polyclonal anti-NHE1 (H-160) was from Santa Cruz Biotechnology, mouse monoclonal anti-NHE1 (4E9) was from Abcam and mouse monoclonal antibody against ß-actin was from Sigma. F-actin and EGFR were visualized in immunofluorescence by using respectively Alexa 488-phalloidin from Molecular Probes, Inc. (Eugene, OR) and Alexa Fluor 405-EGFR (Santa Cruz Biotechnology). Secondary antibodies were anti-mouse (Sigma) and anti-rabbit (Cell Signaling) HRP-linked antibodies, goat anti-mouse conjugated to Alexa Fluor 488 and goat anti-rabbit Alexa Fluor 568 linked (Molecular Probes).

Transient transfection

For NHERF1 overexpression, PANC-1 cells were incubated with 5 µg of plasmid cDNA or empty vector and 15 µl of Lipofectamine transfection reagent 2000 (Invitrogen) in 1 ml of simple DMEM growth medium for 30 min at room temperature (RT) as previously described (Busco et al., 2010). Complete growth medium (10% serum) was added, and 3 ml of this mixture was pipetted onto confluent monolayers onto 6 cm plates and placed in an incubator at 5% CO_2 and 37°C. After 24 hours this mixture was then replaced with fresh complete medium and 24 hours later protein expression was verified by immunoblotting.

NHE1 activity

Intracellular pH was determined spectrofluorimetrically in cells loaded with the acetoxy-methyl ester derivative of the pH-sensitive dye 2,7-biscarboxyethyl-5(6)-carboxyfluorescein (AM-BCECF, Invitrogen). NHE1 activity was determined by measuring the rate of pHi recovery from an acid load produced with the NH4Cl prepulse technique by evaluating the derivative of the slope of the time-dependent pHi recovery (dpHi/dt) as previously described (Cardone et al., 2008). The use of CO2/HCO3 free solutions minimizes the likelihood that sodium-dependent HCO_3 transport was responsible for the observed pHi changes. After each experiment trypan blue exclusion was also measured for each cover slip and when was more than 5% the experiment was not used.

Migration experiments

Migration of PDAC cells, seeded into tissue culture flasks coated with "desmoplastic matrix", was quantified by means of time lapse video microscopy as follows: 4 - 5 hr after seeding, the FCS-containing medium was exchanged for serum-free medium, and the cells were serum-starved overnight. 15 min prior to the start of the experiments the serum-free medium was supplemented with EGF (100 ng/ml) and/or Cariporide (HOE642, 10 µmol/l) as appropriate and motility measured as previously described (Dieterich et al., 2008). Flasks were placed in a heating chamber (37 °C) on the stage of a microscope (Axiovert 25 or 40, Zeiss, Germany) connected to a video camera (Models XC-ST70CE and XC-77CE, Hamamatsu/Sony, Japan). Image acquisition in 5 min intervals was controlled by HiPic or HOKAWO software

(Hamamatsu). Migration during a 3 hr period was quantified as the movement of the cell center with time. The cell center represents the geometric means of equally weighted pixel positions within the cell outlines. Cell speed (μm/min) was calculated as a three point difference quotient and the displacement as the net distance covered within the experiment.

Table 1: Composition of the extracellular matrices

	desmoplastic matrix
RPMI 5x	10.4 g/L
HEPES 5x	10 mmol/L
NaOH	~15 μL 1M NaOH per 1 ml matrix solution; pH7.4
Laminin	120 μg/mL
fibronectin	40 μg/mL
collagen IV	5.4 μg/mL
collagen III	12 μg/mL
collagen I	800 μg/mL
H_2O	add 1 ml

Three-dimensional Matrigel™ growth assay and *in vitro* invasion

For 3D Matrigel™ growth assay, 10^4 cells for each cell line were included in serum-free, 7% Matrigel™ (Becton Dickinson) drops, containing or not EGF (100ng/mL), Cariporide (10μM) or a mixture of both. The drops were then incubated for the indicated times in complete medium ± EGF (100ng/mL), Cariporide (1μM) or both. Media were changed every 2 days with the corresponding fresh media. Images of the hanging drops were acquired and analyzed with a 60X oil objective using a Nikon Eclipse TE 2000S epifluorescence microscope. The colonies within the MatrigelTM matrix were analyzed for size, circularity and density using ImageJ (http://rsb.info.nih.gov/ij/) or stained with DiffQuick (Baxter) and analysed for stain density using Fiji software.

For invasion the upper compartment of trans-well chambers was coated with Matrigel™ and placed in six-well plates. Cells were washed with phosphate buffered saline (PBS) and then detached with 5 mM EDTA in PBS. Detached cells were washed once more in PBS, resuspended in serum-free DMEM and added to the upper compartment of the chamber (10^5 cells/well). Medium with 1.5% serum was placed in the lower compartment of the chambers. To determine the effect of specific inhibitors in the presence or absence of EGF, cells were pretreated with the inhibitor for 1 h before they were added to the chamber, and then fresh inhibitor was added to the well. After a 24 h incubation at 37°C, the cells on the upper surface were completely removed by wiping with a cotton swab and the filter fixed with methanol and stained with crystal violet solution. Cells that had migrated from the upper to the lower side of the filter were counted with a light microscope in 50 fields/filter.

Invadopodia ECM digestion using *in situ* zymography

Experiments were conducted in cells seeded onto a layer of Matrigel™ (diluted to a final concentration of 4 mg/ml) in which quenched BODIPY linked to BSA (DQ-Green-BSA and DQ-Red-BSA) was mixed at a final concentration of 30 μg/ml. The matrix mix was used to cover 12-mm round glass coverslip. Matrigel™ containing the

fluorigenic substrate was allowed to polymerize for 30 min in a humidified incubator at 37°C. Then, $4X10^4$ cells/coverslip were seeded onto the polymerized matrix, and grown overnight in the absence or presence of EGF (100ng/mL), Cariporide (1μM), Erlotinib (5μM, 10μM and 20μM) and EGF (100ng/mL) + Cariporide (1μM)+Erlotinib at the indicated concentations. After the above-mentioned time, cells were fixed with paraformaldehyde 3.7% in PBS and processed for immunofluorescence. Focal ECM digestion produces green fluorescence within a black background. Cells were imaged for F-actin and quantification of ECM degradation was done by counting degradation spots in 10 fields of view (40X objective) in 3 separate experiments for each cell line. The degradation area was determined by using ImageJ 1.41 software and normalized for the number of cells. ECM degradation was analyzed as total focal digestive activity of 100 cells.

Immunofluorescence staining

For immunofluorescence, cells grown on coverslips were rinsed in PBS, fixed with 4% paraformaldehyde in PBS for 15 min at room temperature, permeabilized with 0.5% Triton X-100 in PBS for 5 min and blocked with 5% bovine serum albumin in PBS. After washing with PBS, cells were then incubated with primary antibodies, followed by FITC/TRITC-conjugated secondary antibodies (Molecular Probes), at room temperature. For a better resolution of the plasma membrane, non permeabilized cells were stained with wheat germ agglutinin (WGA)-TRITC conjugated (100 mg/ml) (Sigma) that selectively recognizes sugar residues on the plasma membrane. Slides were mounted with Vectashield antifade solution (Vector Laboratories, Burlingame, CA, USA) and observed with a Nikon TE 2000S epifluorescence microscope equipped with a MicroMax 512BFT charge-coupled device (CCD) camera (Princeton Scientific Instruments, Monmouth Junction, NJ) or with a Leica TCS SP5 II microscope equipped with a laser-scanning confocal unit containing a He-Ne argon laser (Leica). Specimens were viewed through a Planapo 63X/1.25 oil immersion objective and images were acquired by LAS-AF version 2.2.1 build 4842 software.

Coimmunoprecipitation and Immunoblot Analysis

Interactions of NHERF1 with EGFR and NHE1 were analyzed in PANC-1-1 cells transiently transfected with WT-NHERF1 or the respective empty vector and stimulated or not with EGF for the indicated times 10, 30, 60 minutes and overnight. After treatment monolayers were washed two times with ice-cold phosphate buffered saline (PBS) and then lysed in ice-cold coimmunoprecipitation lysis buffer (50 mM Tris, pH 7.5, 150 mM NaCl, 1% NP-40, 0.5% sodium deoxycholate, 100 μM Na_3VO_4, and 1 mM NaF, protease inhibitors) and homogenated by five passes through a 20-gauge needle to obtain the total cell homogenate. An aliquot was removed for the determination of total cellular protein. Approximately 300 μg of total cellular protein was incubated overnight on a rotator with 2 μg of each of the primary antibodies. Fifty microliters of resuspended volume of PureProteome Protein A/G Magnetic Beads (Millipore) were then added to each mix cellular homogenate-antibody and incubated at 4°C on a rotator for three hours. Immunoprecipitates were collected by centrifugation at 2500 rpm for 5 min at 4°C. Supernatant was carefully aspirated and discarded, and the pellet was washed four times with 1 ml of lysis buffer, each time repeating the centrifugation step above. After the final wash, the pellet was resuspended in 40 μl of SDS sample buffer (6.25 mM Tris-HCl, pH 6.8, containing 10% [vol/vol] glycerol, 3 mM SDS, 1% [vol/vol] 2-mercaptoethanol, and

0.75 mM bromophenol blue) and was run on 10% SDS-PAGE and analyzed by Western blotting with a policlonal antibody against EGFR (D38B1, Cell Signaling Technology), monoclonal anti-NHERF1 (BD Biosciences Transduction Laboratories) or NHE1 (rabbit polyclonal anti-NHE1 (H-160), Santa Cruz Biotechnology.

Orthotopic implantation of human pancreatic tumor cell lines

Severe combined immunodeficient mice (SCID mice), strain C.B-17/ Ztm-scid of box sexes or nude mice, strain NMRI-Fox1 nu/nu, were used for tumor cell implantation in accordance with the Declaration of Helsinki protocols as described previously (Alves et al., 2001). For orthotopic transplantation, general anesthesia was performed by intraperitonel application using a mixture of ketamine (75 – 100 mg/ kg) and xylazin (15 – 20 mg/kg). A median laparotomy was performed, approximately 1 cm in length, the peritoneum opened and the pancreas carefully exposed by applying gentle traction at the stomach and duodenum. Aliquots of 1 x 10^6 pancreatic tumor cells in a volume of 15 µl PBS were injected with an insulin syringe, 29 gauge × 1/2 (Becton Dickinson, Heidelberg, Germany) very slowly into the duodenal lobe of the pancreas through the pancreatic serosa into the pancreatic tissue. The cells were implanted so as to visible infiltrate the pancreatic tissue. The needle was slowly withdrawn after one min delay. The pancreas was then returned to the abdominal cavity and the incision was closed in two layers using a continious Vicryl suture (Metric 1.5, Ethicon, Norderstedt, Germany) for the peritoneum and an interrupted suture for the skin.

At the end of the experiments autopsies were performed and the abdomen and thoracic cavity were examined systematically for the presence of metastases. All findings, complications, such as biliary and stomach obstruction, ascites, grade of invasion into the surrounding tissue and the size, numbers and location of metastases were recorded. The three dimensions of the tumor, the width, length and height of the pancreatic tumor were measured and the volumes of the primary growing tumors were then calculated according to the formula 0.5 x length x width x height. The pancreatic tumor mass including the attached organs, metastases, nodules suspicious of being metastasis, lung, liver, spleen, kidneys, adrenal glands, diaphragm, different parts of the intestine, bladder and the male and female genitals organs were excised and placed in phosphate-buffered 4% formalin for 16 hours at room temperature and embedded in paraffin. 2.5 µm tissue sections were obtained.

Immunohistofluorescent staining of surgical specimens

Sections were immunostained with monoclonal antibody against EGFR (Alexa Fluor 405-EGFR, Santa Cruz Biotechnology), rabbit polyclonal antibody against NHERF1 (Affinity Bio Reagents) and with monoclonal antibody against NHE1 (clone 4E9, from Abcam). The latter were followed by exposure to Alexa 488- or Alexa 568-labeled secondary antibodies (Molecular Probes). Each section was also examined for hematoxylin and eosin staining. Specimens were viewed through a Plan Fluor 20X objective by the use of a Nikon TE 2000S epifluorescence microscope equipped with a MicroMax 512BFT charge-coupled device (CCD) camera (Princeton Scientific Instruments, Monmouth Junction, NJ) and analyzed by ImageJ (http://rsb.info.nih.gov/ij/).

Data mining from gene expression data.

To explore the potential contribution of NHE1 in EGFR function in PDAC, we analysed differential gene expression using a Microarray U133 A/B Affymetrix

GeneChip data set containing gene expression values derived from microdissected tissues including pancreatic tumor and normal epithelium, stromal tissue, stromal chronic pancreatitis specimens and from a set of pancreatic tumor, normal and stellate cell lines (6, 7). The data set was analyzed with the EGAN (Exploratory Gene Association Networks) program (8) for Association Nodes in a subset of ion transporter proteins and signal transduction molecules. The list of genes interrogated in the analysis came from the IonTraC consortium (*www.iontrac.uni-muenster.de*).

Statistical Procedures

Data correspond to at least three independent experiments, each of which was done in triplicate. Results are presented as means ± standard error (SE). The data for each condition were subject to analysis of variance (ANOVA) followed by Dunnet post-hoc test when comparing three or more conditions or evaluated using Student's t-test when comparing only two conditions. Significant differences were considered with values of $p < 0.05$.

The results of single and combined treatments with erlotinib and cariporide on 3D growth were analyzed according to the method of Chou and Talalay (1984) (Chou and Talalay, 1984). The resulting combination index (CI) represents a quantitative measure of the degree or type of interaction between different drugs, with CI > 1.1, CI = 0.9-1.1, and CI < 0.9 indicating antagonistic, additive, and synergistic effects, respectively. This analysis takes into account both the potency (IC_{50}) and shape of the dose-response curve. One of the major objectives of having synergistic drug combination is to reduce the dose of the drug used, thereby reducing the toxicity while maintaining efficacy. The Dose Reduction Index (DRI) is a measure of how many -fold the dose of each drug in a synergistic combination may be reduced at a given effect level compared with the doses of each drug alone (Chou, 2006). IC_{50}, Combination Index (CI) and Dose Reduction Index (DRI) were calculated with the CalculSyn Software.

The DRI value for each corresponding drug is calculated simply by inverting each term of the equation for CI. Thus, for two-drug combinations:

$$CI = D1/Dx1 + D2/Dx2 = 1/(DRI)1 + 1/(DRI)2 \quad (1)$$

Therefore: $(DRI)1 = Dx1/D1$ and $(DRI)2 = Dx2/D2$ (2)

The DRI is important in clinical situations, since dose reduction would lead to reduced patient toxicity while maintaining therapeutic efficacy. Although DRI > 1 is beneficial, it does not necessarily indicate synergism because, from the above equation, an additive effect or even slight antagonism may also lead to DRI >1 (ie. if drug A and drug B each inhibit 50%, and if (0.5A + 0.5B) also inhibits 50% and if both drugs have no overlapping toxicity toward the host, then indeed DRI ≈1 may still be beneficial). Higher DRI values indicate a greater dose reduction for a given therapeutic effect, but does not necessarily always indicate synergism, as shown by the mathematical relationship of CI and DRI given in eq. 1 above.

Alves, F., Contag, S., Missbach, M., Kaspareit, J., Nebendahl, K., Borchers, U., Heidrich, B., Streich, R., and Hiddemann, W. (2001). An orthotopic model of ductal adenocarcinoma of the pancreas in severe combined immunodeficient mice representing all steps of the metastatic cascade. Pancreas *23*, 227-235.

Busco, G., Cardone, R. A., Greco, M. R., Bellizzi, A., Colella, M., Antelmi, E., Mancini, M. T., Dell'Aquila, M. E., Casavola, V., Paradiso, A., and Reshkin, S. J. (2010). NHE1 promotes invadopodial ECM proteolysis through acidification of the peri-invadopodial space. FASEB J *24*, 3903-3915.

Cardone, R. A., Busco, G., Greco, M. R., Bellizzi, A., Accardi, R., Cafarelli, A., Monterisi, S., Carratu, P., Casavola, V., Paradiso, A., *et al.* (2008). HPV16 E7-dependent transformation activates NHE1 through a PKA-RhoA-induced inhibition of p38alpha. PLoS One *3*, e3529.

Chou, T. C. (2006). Theoretical basis, experimental design, and computerized simulation of synergism and antagonism in drug combination studies. Pharmacol Rev *58*, 621-681.

Chou, T. C., and Talalay, P. (1984). Quantitative analysis of dose-effect relationships: the combined effects of multiple drugs or enzyme inhibitors. Adv Enzyme Regul *22*, 27-55.

Dieterich, P., Klages, R., Preuss, R., and Schwab, A. (2008). Anomalous dynamics of cell migration. Proc Natl Acad Sci U S A *105*, 459-463.

Supplemental Figure Legends and Figures

FIGURE S1. Macroscopic appearance of primary pancreatic tumors and tumor spread in orthotopic pancreatic tumor models.

The tumors grew within the pancreas, infiltrated the normal pancreatic tissue and formed a localised tumor within the pancreas with signs of invasion into the neighbouring organs or tumor spread at the time of section as demonstrated in Fig. Invasion, metastasis and complications of the tumors are listed in Table S1. All animals also developed peritoneal tumors at the scar, the site of surgical incision.

FIGURE S2. Typical intracellular pH recovery in the panel of the PDAC cells acidified by ammonium prepulse in nominally HCO_3-free media. Cells were perfused with 20 mM NH_4-HEPES-buffered solution, followed by washout in NH_4-free and Na^+-free media (N-methyl-D-glucamine (NMDG) was used as a substitute for Na^+). Recovery from acidification was dependent on the presence of extracellular Na^+. Recovery was measured in the absence (CTR) or presence of 500nM cariporide (HOE694). Each trace is the representative of different types of PDAC cells. To then measure the activation of NHE1 by the EGFR, cells from each cell line were perfused with 20 ng/ml EGF for 10 min followed by measurements of pHi recovery as above.

FIGURE S3. Invadopodial focal ECM degradation measured by an in vitro fluorescent-Matrigel degradation assay. Cells were seeded on coverslips coated with

Matrigel (4mg/ml) and BSA-BODIPY (30μg/ml) and incubated at 37° C for 24 hr. Panels show representative pictures of proteolytic degradation in the Matrigel matrix in green (BSA-BODIPY) and actin immunofluorescence in red (bar, 10 μm). Inserts: Confocal immunofluorescent localization shows invadopodia (arrows) visible as F-actin dots co-localizing with cortactin and overlapping with areas of ECM degradation. Bar, 10μm.

FIGURE S4. Basal expression levels of NHERF1 in the four PDAC cell lines. Protein loading normalized to β-actin levels.

FIGURE S5. Proteasome/Ubquitin: Representitive Western Blots showing the effect of the pre-incubation with the proteasome inhibitor MG132 on NHERF1, EGFR and total ubiquitin-conjugated proteins in control (A) and WT-NHERF1 overexpressing (B) PANC-1 cells. Protein loading normalized to β-actin levels.

FIGURE S6. Immunoprecipatation (A) and Immunofluorescence (B) in WT-NHERF1 overexpressing PANC-1 cells.

FIGURE S7. Confocal reconstruction of lipid raft plasma membrane complexes. To better visualize the structure of the protein-protein complexes, we utilized confocal microscopy. Confocal images in axial planes taken at the bottom of the cells (XY) of a typical cell show EGFR (blue), WGA (red) and Caveolin (green) localization in complex sub plasma membrane structures. For the field, XZ zoomed sections of the above representative regions of interest (white boxes) are shown at the side. Scale bars = 10 μ m (XY) and 5 μ m (XZ).

Figure S1

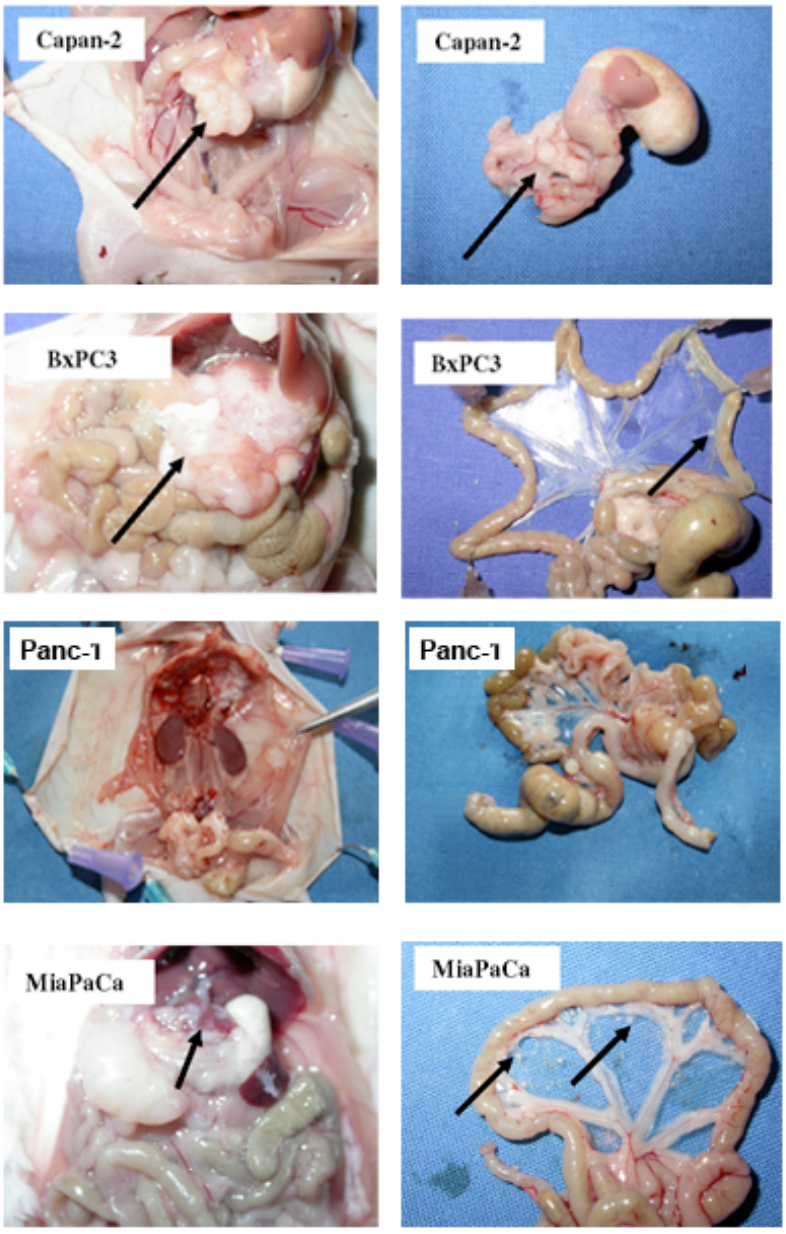

Figure S2

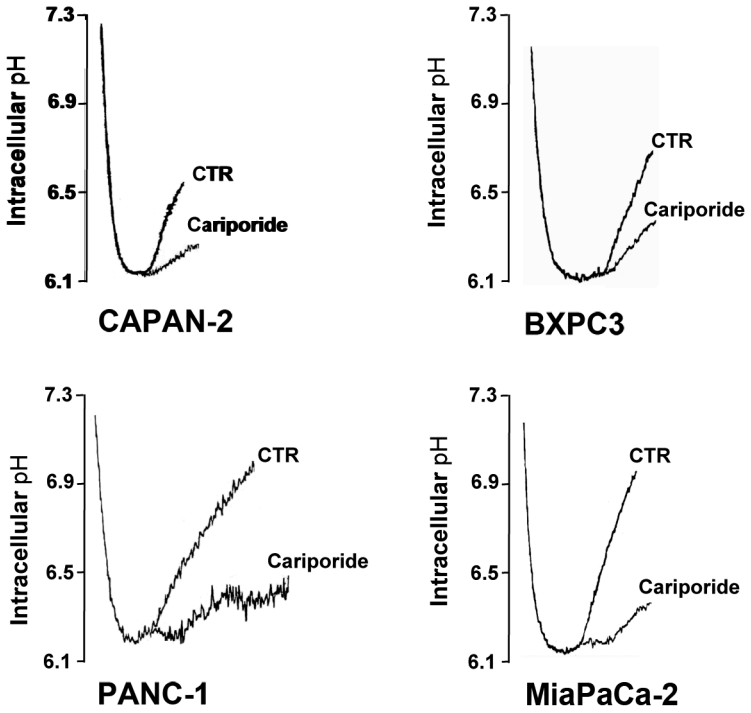

Figure S3

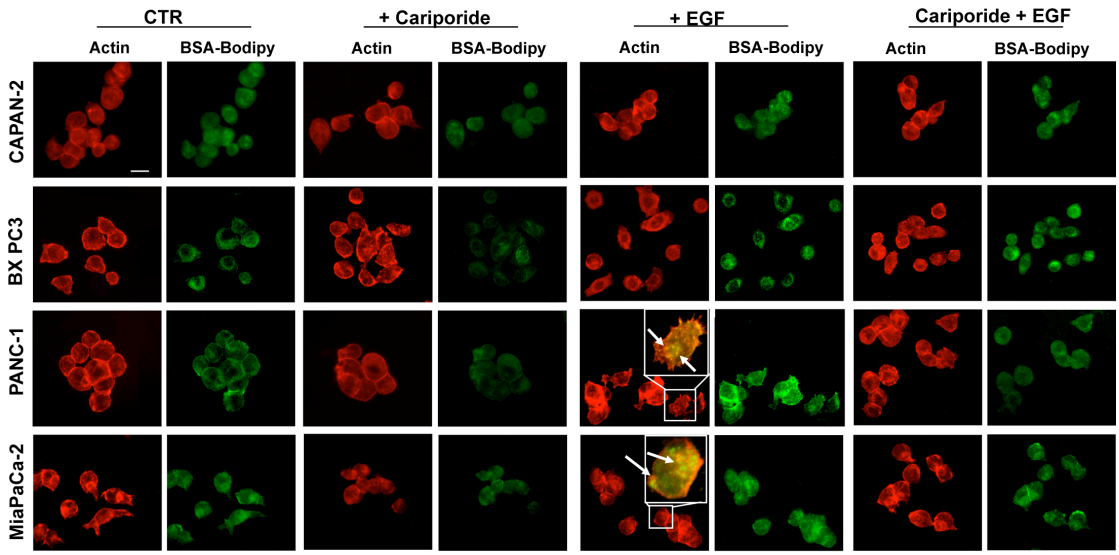

Figure S4

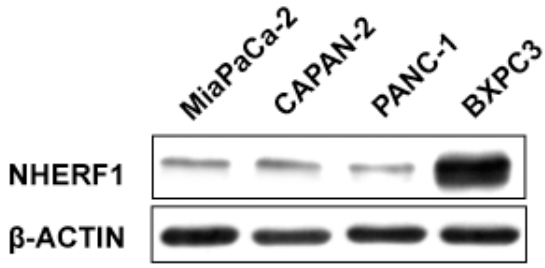

Figure S5

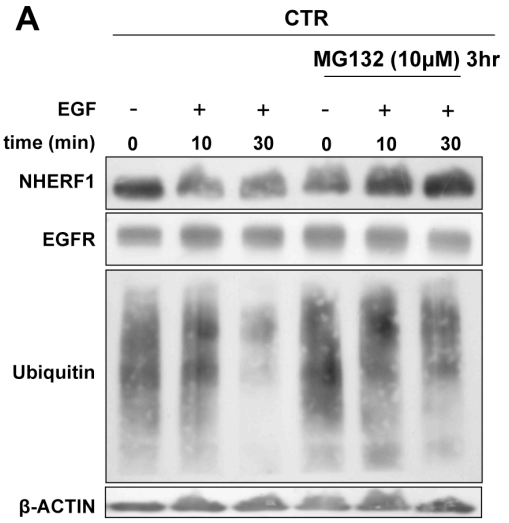

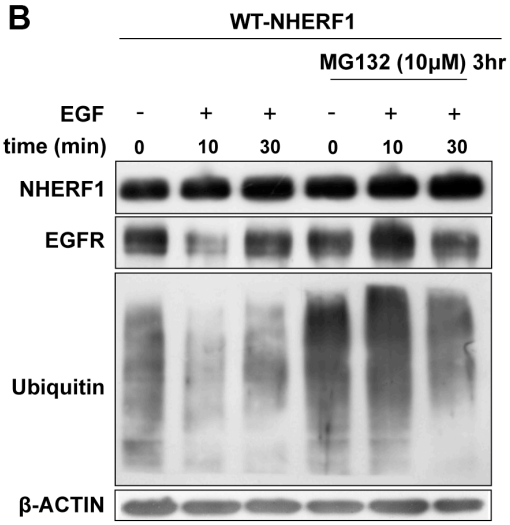

Figure S6

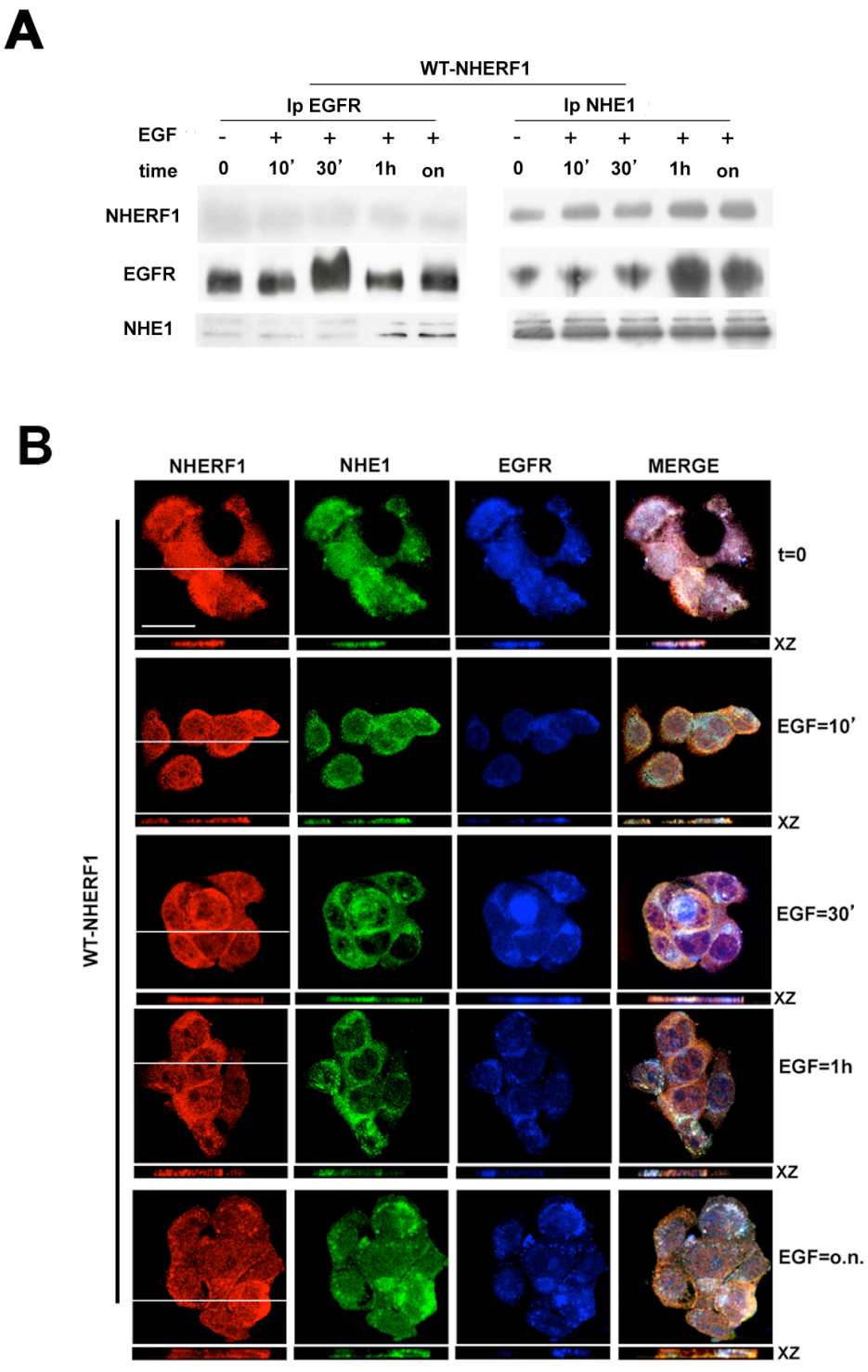
A
WT-NHERF1
Ip EGFR
Ip NHE1
EGF
time
0
10'
30'
1h
on
NHERF1
EGFR
NHE1
B
NHERF1
NHE1
EGFR
MERGE
WT-NHERF1
t=0
EGF=10'
EGF=30'
EGF=1h
EGF=o.n.
XZ

Figure S7

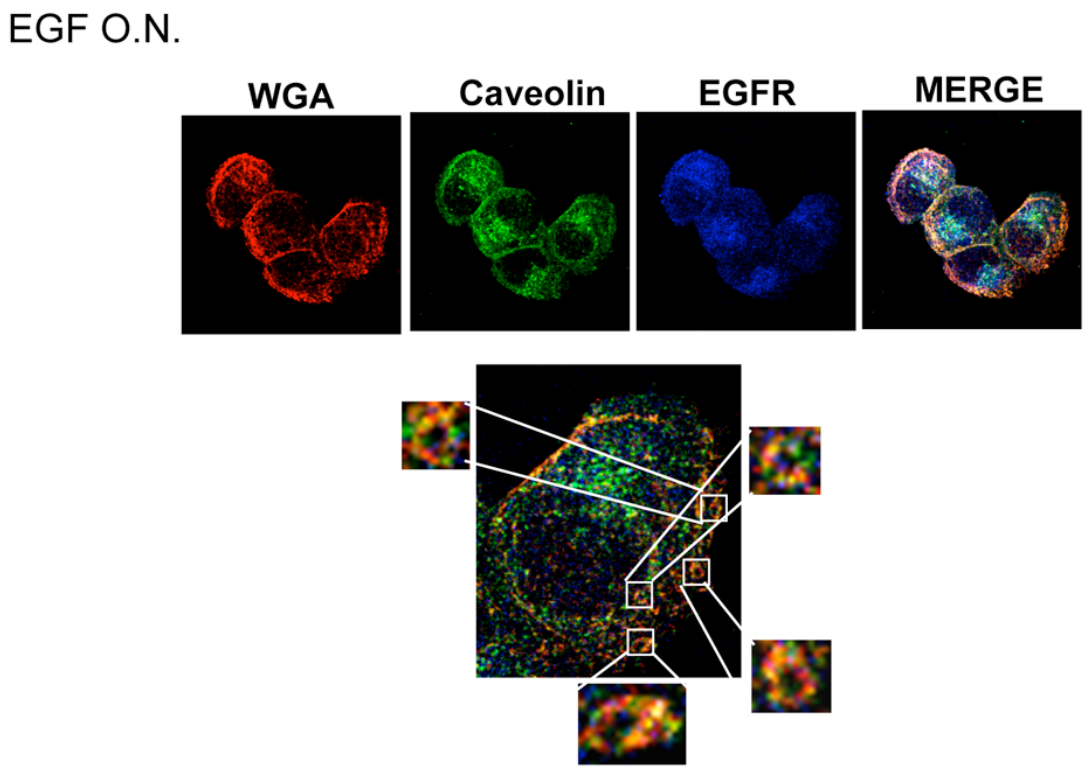

Table 1. Invasion and Metastases of orthotopically implanted cells

	MiaPaCa-2	BXPC3	Capan-2	Panc-1
Invasion				
Stomach	+	+	+	+
Duodenum	+	+	-	+
Liver (porta hepatis)	-	+	-	+
Spleen	-	-	-	-
Complications				
Biliary obstruction	-	-	-	-
Stomach obstruction	-	+	-	+
Ascites	-	-	-	-
Macroscopic appearance Metastases				
Mesentery (1–3 met.)		+		
Mesentery (3 -10 met.)				+
Mesentery (> 10 met.)	+ (small)			
Liver	-	-	-	-
Diaphragm	-	+	-	+
scar	+	+	+	+
	V_m= 36 mm^3	V_m= 550 mm^3	V_m= 380 mm^3	V_m= 365 mm^3

At the end of the experiments autopsies were performed and the abdomen and thoracic cavity were examined systematically for the presence of metastases. All findings, complications, such as biliary and stomach obstruction, ascites, grade of invasion into the surrounding tissue and the size, numbers and location of metastases were recorded. The three dimensions of the tumor, the width, length and height of the pancreatic tumor were measured and the volumes of the primary growing tumors were then calculated according to the formula 0.5 x length x width x height. The pancreatic tumor mass including the attached organs, metastases, nodules suspicious of metastasis, lung, liver, spleen, kidneys, adrenal glands, diaphragm, different parts of the intestine, bladder and the male and female genital organs were excised and placed in phosphate - buffered 4% formalin for 16 hours at room temperature and embedded in paraffin. 2.5 μm tissue sections were obtained. Vm is the mean volume of tumor formed at the scar.